Myeloid cell dynamics correlating with clinical outcomes of severe COVID-19 in Japan

Tomohiro Takano,[1] Takayuki Matsumura,[1,*] Yu Adachi,[1] Kazutaka Terahara,[1] Saya Moriyama,[1] Taishi Onodera,[1] Ayae Nishiyama,[1] Ai Kawana-Tachikawa,[2] Shoji Miki,[2] Kaori Hosoya-Nakayama,[2] Midori Nakamura-Hoshi,[2] Sayuri Seki,[2] Natsuo Tachikawa,[3] Yukihiro Yoshimura,[3] Nobuyuki Miyata,[3] Hiroshi Horiuchi,[3] Hiroaki Sasaki,[3] Kazuhito Miyazaki,[3] Noriko Kinoshita,[4] Tsutomu Sudo,[4] Yutaro Akiyama,[4] Rubuna Sato,[4] Tadaki Suzuki,[5] Tetsuro Matano,[2] and Yoshimasa Takahashi[1,*]

[1]Department of Immunology, National Institute of Infectious Diseases, 1-23-1 Toyama, Shinjuku-ku, Tokyo, 162-8640, Japan.

[2]AIDS Research Center, National Institute of Infectious Diseases, 1-23-1 Toyama, Shinjuku-ku, Tokyo, 162-8640, Japan.

[3]Department of Infectious Diseases, Yokohama Municipal Citizen's Hospital, 1-2 Mitsuzawanishimachi, Kanagawa-ku, Yokohama, Kanagawa, 221-0855, Japan.

[4]Disease Control and Prevention Center, National Center for Global Health and Medicine, 1-21-1 Toyama, Shinjuku-ku, Tokyo, 162-8655, Japan.

[5]Department of Pathology, National Institute of Infectious Diseases, 1-23-1 Toyama, Shinjuku-ku, Tokyo, 162-8640, Japan.

*Correspondence:

Takayuki Matsumura

Department of Immunology, National Institute of Infectious Diseases, 1-23-1 Toyama, Shinjuku-ku, Tokyo, 162-8640, Japan

Email: matt@niid.go.jp, Phone: +81-3-5285-1111

Yoshimasa Takahashi

Department of Immunology, National Institute of Infectious Diseases, 1-23-1 Toyama, Shinjuku-ku, Tokyo, 162-8640, Japan

Email: ytakahas@niid.go.jp, Phone: +81-3-5285-1111

Abstract

An expanded myeloid cell compartment is a hallmark of severe coronavirus disease 2019 (COVID-19). However, data regarding myeloid cell expansion have been collected in Europe, where the mortality rate by COVID-19 is greater than those in other regions including Japan. Thus, characteristics of COVID-19-induced myeloid cell subsets remain largely unknown in the regions with low mortality rates. Here, we analyzed cellular dynamics of myeloid-derived suppressor cell (MDSC) subsets and examined whether any of them correlate with disease severity and prognosis, using blood samples from Japanese COVID-19 patients. We observed that polymorphonuclear (PMN)-MDSCs, but not other MDSC subsets, transiently expanded in severe cases but not in mild or moderate cases. Contrary to previous studies in Europe, this subset selectively expanded in survivors of severe cases and subsided before discharge, but such transient expansion was not observed in non-survivors in Japanese cohort. Analysis of plasma cytokine/chemokine levels revealed positive correlation of PMN-MDSC frequencies with interleukin 8 (IL-8) levels prior to the cell expansion, indicating the involvement of IL-8 on recruitment of PMN-MDSCs to peripheral blood following the onset of severe COVID-19. Thus, our data indicates that transient expansion of the PMN-MDSC subset results in improved clinical outcome. Thus, this myeloid cell subset may be a predictor of prognosis in cases of severe COVID-19 in Japan.

Keywords

SARS-CoV-2, Innate immunity, Myeloid-derived suppressor cell, Cytokine, Chemokine

Graphical_abstract

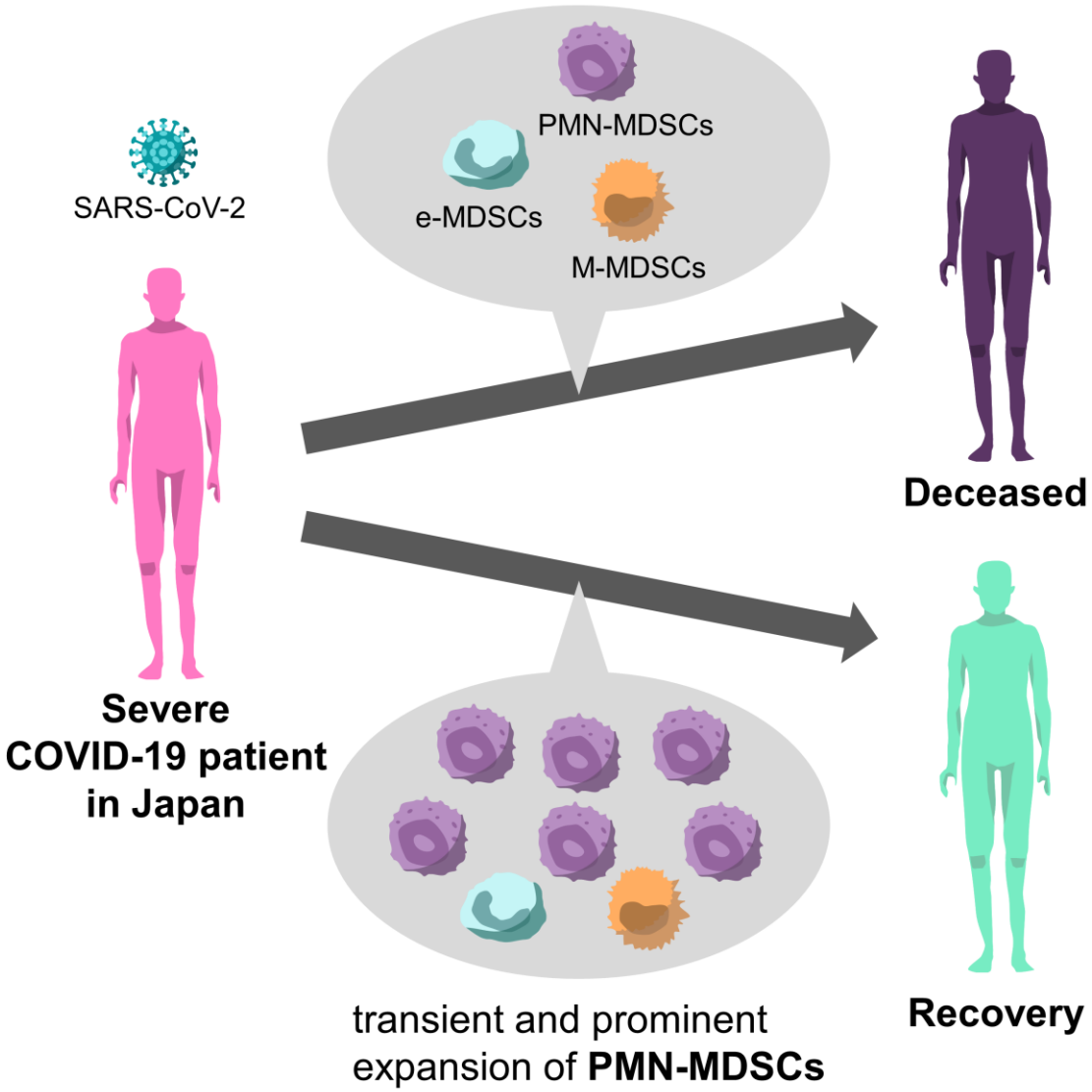

Introduction

In December 2019, coronavirus disease 2019 (COVID-19), caused by severe acute respiratory syndrome coronavirus 2 (SARS-CoV-2), was first reported in Wuhan, Hubei Province, China. The virus spread rapidly, causing a global pandemic (1-5). Although most COVID-19 patients are asymptomatic or present with mild clinical symptoms that resemble seasonal coronavirus diseases, 19% of patients suffer from severe or critical disease with 2.3% mortality (6). The countermeasure for the pandemic is to protect those who are at greater risk of death from COVID-19, including the elderly and those with comorbidities, such as hypertension, diabetes, and cardiac/pulmonary diseases (6,7). Notably, the mortality rate is obviously lower in Asia than in US and Europe (8), but it remains unclear why the Asian population is resistant to COVID-19-related morbidity, although several hypotheses have been put forth.

Myeloid-derived suppressor cells (MDSCs) are a heterogeneous population of immature myeloid cells that mediate immune suppression and are generated during a large array of pathogenic conditions ranging from cancer to obesity (9). In humans, MDSCs consist of at least three groups of cells, namely, early stage MDSCs (e-MDSCs), monocytic MDSCs (M-MDSCs), and polymorphonuclear MDSCs (PMN-MDSCs). These have been found in peripheral blood mononuclear cells (PBMCs), in addition to bone marrow and inflammatory tissues (9). Various infectious diseases have been reported to induce MDSCs, including bacterial, fungal, parasitic, and viral infections (10); however, their roles in disease pathogenesis are still unclear. Notably, individuals with the aforementioned risk factors for COVID-19 are prone to sustain increased frequencies of MDSCs (9,11). In addition, elevated levels of interleukin 6 (IL-6) and IL-8, well-known inducers of MDSCs (12-14), are observed in severe cases of COVID-19 (15,16).

This information suggests a possible link between MDSCs and COVID-19. The expansion of MDSCs and MDSC-like cells has been repeatedly observed in severe COVID-19 patients by several research groups from European countries (17-21). However, the previous results may not be directly applicable in other regions where the mortality rate is lower. In this study, we describe the transient but prominent expansion of the PMN-MDSC subset in survivors, but not in non-survivors, of severe COVID-19 in Japan. Our data suggest the beneficial role of PMN-MDSC subset, which potentially suppress excessive inflammation during recovery from severe COVID-19 in Japan.

Methods

Ethics approval and consent to participate

This study protocol was approved by the National Institute of Infectious Diseases Ethic Review Board for Human Subjects (Permit numbers: 1107 and 1111), the ethics committee of Yokohama Municipal Citizen's Hospital (Permit number: 20-03-04), and the ethics committee of Center Hospital of the National Center for Global Health and Medicine (Permit number: NCGM-A-003535-00). All participants provided written informed consent in accordance with the Declaration of Helsinki.

Human subjects

This study enrolled 40 patients with mild (n = 12), moderate I (n = 7), moderate II (n = 8), and severe (n = 13) COVID-19 at two hospitals in Japan (Yokohama Municipal Citizen's Hospital and Center Hospital of the National Center for Global Health and Medicine), as well as seven healthy donors. The severity of symptoms was stratified according to the third edition of the medical guidelines of COVID-19 provided by the Japanese Ministry of Health,

Labor and Welfare (22). Mild cases were defined as having no pneumonia with minimal or no clinical symptoms. Moderate I and moderate II cases were defined by the presence of pneumonia without and with the need for supplemental oxygen (93% < SpO_2 < 96%, moderate I; $SpO_2 \leq 93\%$, moderate II), respectively. Severe cases were defined as having pneumonia and respiratory distress requiring ICU admission or ventilator use. Clinical characteristics of patients and time points of blood sampling are provided in Supplementary Table 1.

Preparation of PBMCs and plasma

Blood samples were collected from the COVID-19 patients and healthy donors using a BD Vacutainer® CPT™ Tube (BD Biosciences, Franklin Lakes, NJ) and centrifuged for 20 min at 1500–1800 g at 23 °C. Following centrifugation, the cells and supernatant were isolated as PBMCs and plasma, respectively. PBMCs were washed with PBS (FUJIFILM Wako Pure Chemical Corporation, Osaka, Japan), cryopreserved in CELLBANKER 1 plus (ZENOAQ RESOURCE, Fukushima, Japan), and stored at -135 °C until further analysis. Plasma was stored at -80 °C until further analysis. For analysis, the cryopreserved PBMCs were thawed using RPMI 1640 (FUJIFILM Wako Pure Chemical Corporation) containing 10% fetal bovine serum (Nichirei Biosciences, Tokyo, Japan), 2 mM glutamine (FUJIFILM Wako Pure Chemical Corporation), 50 µM 2-mercaptoethanol (Thermo Fisher Scientific, Waltham, MA), 100 U/ml penicillin (FUJIFILM Wako Pure Chemical Corporation), and 100 µg/ml streptomycin (FUJIFILM Wako Pure Chemical Corporation).

Flow cytometry

PBS (Nacalai Tesque, Kyoto, Japan) containing 0.5% bovine serum albumin (Roche Diagnostics, Basel, Switzerland) and 5 mM EDTA (Thermo Fisher Scientific) was used as the antibody staining buffer and wash buffer. PBMCs were incubated with Human TruStain FcX (BioLegend, San Diego, CA) for 10 min at 23 °C to avoid binding of nonspecific antibodies (Fc blocking). Following washing, PBMCs were stained with CD11b-FITC (clone ICRF44; BioLegend), CD14-BV650 (clone M5E2; BD Biosciences), CD15-APC (clone W6D3; BioLegend), CD33-APC/Cyanine7 (clone P67.6; BioLegend), CD33-BV510 (clone WM53; BD Biosciences), and HLA-DR-PE/Cy7 (clone G46-6; BD Biosciences) for 20 min at 4 °C. Additionally, 7-aminoactinomycin D (Sigma-Aldrich, St Louis, MO, USA) was used simultaneously to stain dead cells. Following thorough washing, specimens were analyzed using a FACSAria III flow cytometer (BD Biosciences). Data obtained from flow cytometry were analyzed using FlowJo v10.6.1 (BD Biosciences).

Cytokine/chemokine quantification

Plasma cytokines/chemokines were measured using a cytometric bead array kit (BD Biosciences) according to the manufacturer's instructions. Data were acquired using a FACSCalibur flow cytometer (BD Biosciences) and analyzed using FCAP Array Software Version 3.0 (BD Biosciences).

Statistical analysis

Data comprising the flow cytometric frequencies of cells were compared with two-way ANOVA with post-hoc Tukey's honest significant difference test. For plasma cytokine levels below the detection limit, the value was set to 0.01 pg/ml. Cytokine concentrations were compared with one-way ANOVA with post-hoc Tukey's honest significant difference test.

Statistical significance was set at $^{**}p < 0.01$, $^{***}p < 0.001$, and $^{****}p < 0.0001$. Spearman correlations between plasma cytokine concentrations and cell frequencies were identified in all specimens. Correlations with $r > 0.4$ or $r < -0.4$ and $p < 0.01$ were considered significant. A simple regression line was shown for a significant correlation. GraphPad Prism version 9.0 (GraphPad Software, San Diego, CA, USA) was used for all statistical analyses and graphical representations.

Data availability

All scripts used in this manuscript are available upon reasonable request.

Results and Discussion

Three MDSC subsets (e-MDSCs, M-MDSCs, and PMN-MDSCs) in PBMCs were analyzed using flow cytometry (Fig. 1). e-MDSCs, M-MDSCs, and PMN-MDSCs were phenotypically defined as $CD3^{-}CD19^{-}CD56^{-}HLA\text{-}DR^{-}CD11b^{+}CD33^{+}CD14^{-}CD15^{-}$, $CD3^{-}CD19^{-}CD56^{-}HLA\text{-}DR^{-}CD11b^{+}CD33^{+}CD14^{+}CD15^{-}$, and $CD3^{-}CD19^{-}CD56^{-}HLA\text{-}DR^{-}CD11b^{+}CD33^{+}CD14^{-}CD15^{+}$, respectively (Fig. 1A and 1B) (9,23). PMN-MDSCs are found in the low-density Ficoll-gradient fraction of PBMCs, whereas granulocytes are isolated from the high-density fraction (9). In this study, to avoid granulocyte contamination, such cells were removed using a BD Vacutainer® CPT™ Tube (BD Biosciences, Franklin Lakes, NJ) based on Ficoll-gradient centrifugation. The frequencies of each MDSC subset among live PBMCs were tracked with time after symptom onset (Fig. 1C and Supplementary Figure 1). The results were plotted for the first 3 weeks after symptom onset to compare data based on similar time points for cellular analysis in all groups (Fig. 2). Reproducing findings in recent publications (18-20), the frequencies of PMN-MDSCs, but not e-MDSCs or M-MDSCs, dramatically increased in severe COVID-19 (Fig. 1C, 2, and Supplementary Figure 1). Further extending previous findings, we found that the increase in PMN-MDSCs was

transient, and the frequencies of PMN-MDSCs returned to basal levels during the recovery phase before discharge (Fig. 1C). Together, we conclude that the PMN-MDSC subset emerges in the peripheral blood stream in correlation with disease severity and declines by the time of discharge.

Subdivision of severe cases into survivors and non-survivors gives us important indications as to how the increased MDSC subset contributes to the clinical outcome and whether this subset is beneficial or detrimental to the prognosis. Notably, a selective increase of the PMN-MDSC subset, but not the e-MDSC subset or the M-MDSC subset, in survivors of severe COVID-19 was observed, whereas the PMN-MDSC subset remained unchanged in non-survivors even in severe COVID-19 (Fig. 1C and 2).

To gain insight into the cytokines/chemokines that affect MDSC dynamics, we subsequently analyzed plasma levels of cytokines and chemokines, including IL-1β, IL-2, IL-4, IL-5, IL-6, IL-8, IL-10, IL-12 p70, IL-17F, granulocyte colony-stimulating factor (G-CSF), granulocyte-macrophage colony-stimulating factor (GM-CSF), interferon α (IFN-α), IFN-γ, IFN-γ-induced protein 10 (IP-10), monocyte chemotactic protein 1 (MCP-1), monokine induced by IFN-γ (MIG), macrophage inflammatory protein (MIP)-1α, and tumor necrosis factor (TNF)-α, in all donors (Fig. 3). Compared to healthy controls, most cytokines/chemokines, except IL-8, were not significantly elevated in cohorts of this study. We observed a significant and selective increase in IL-8 levels and PMN-MDSC subset from survivors of severe cases (Fig. 2 and 3). These results imply a link between IL-8 and PMN-MDSC induction. In agreement with this, we found that IL-8 levels and PMN-MDSC frequency were positively correlated (Fig. 4). Given the chemoattractant activity of IL-8 in the PMN-MDSC subset (14), PMN-MDSCs might be recruited into peripheral blood by IL-8 following the onset of severe COVID-19.

The current study still has a few limitations. 1) The sample size of this study was small due to a limited availability of patients. A recent cohort study in the United States revealed that male patients had higher plasma levels of innate immune cytokines including IL-8 along with more robust induction of non-classical monocytes (24). Therefore, the sex difference between the groups of severe-discharged (7 males and 1 female) and deceased (4 females and 1 male) patients might affect any events in induction of PMN-MDSCs (Supplementary Table 1). It is important to accumulate more data before generalizing the results in this study. 2) Frozen PBMCs were used in this study. We recognize that total cell numbers would be lowered by freezing and thawing process. However, in order to find the myeloid subsets that correlate with disease severity, it is acceptable to compare the frequency of cells in each MDSC subset among the patients. Under these limitations, we revealed the transient expansion of the PMN-MDSC subset as a survival-specific event that coincides with recovery from the disease in a Japanese cohort. MDSCs are heterogeneous myeloid cell subsets that expand proportionally to the severity of inflammatory diseases. Indeed, several groups have recently reported the expansion of MDSC subsets in severe COVID-19 patients (17-20), but the link between MDSC subsets and clinical outcome largely unknown, owing to limitations in experimental design. Our data indicates a beneficial role of the PMN-MDSC subset, contributing to recovery from severe COVID-19 in Japan.

Contrary to our results, recent Italian cohort study observed higher frequency of the PMN-MDSCs in non-survivors than those in survivors at the time of admission (21). It was, therefore, proposed that early expansion of PMN-MDSCs may inhibit protective immune response, thus contributing to worsening of disease. On the other hand, delayed and transient expansion of PMN-MDSC subset in survivors of our Japanese cohort study raises an alternative possibility that this cell subset may inhibit harmful immune responses caused in severe COVID-19 cases. The variation in outcomes of these studies could be caused by the

differences in experimental design and methods including the sample preparation. However, it is also tempting to speculate that several genetic factors may contribute to the differences (25). Pre-existence of cross-protective immunity and/or trained immunity by previous seasonal coronavirus infections and vaccinations, such as Bacillus Calmette-Guérin vaccine, may also have role to play here (26).

MDSCs are considered to play a harmful role in cancer and several infectious diseases (9,10). However, they have a beneficial role not only in generating tolerance in autoimmune diseases and allograft transplantation but also in providing protection against sepsis (27-29). During severe COVID-19, neutralizing antibody responses arise slower than they do against other acutely infectious viruses such as influenza virus. Therefore, the period prior to the induction of acquired immunity might be a decisive point for the clinical outcome of severe cases, in which the containment of viral replication without hyperinflammation is essential. Along the same line, it has been demonstrated that the anti-inflammatory drugs dexamethasone and anti-IL-6 receptor monoclonal antibody reduce the mortality rate of severe COVID-19 cases (30-33). Thus, we propose that the delayed and transient expansion of the PMN-MDSC subset may be beneficial for the clinical outcome by reducing the severe lung inflammation/sepsis associated with COVID-19 (26) and may be a predictor of prognosis in cases of severe COVID-19, at least in Japanese cohorts.

Funding

This work was supported by the Japan Agency for Medical Research and Development (grant numbers: JP19fk0108104 and JP20fk0108104 to T. Suzuki and Y.T.).

Acknowledgments

We thank Michio Aiko, Rutaro Iwabuchi, Yasuko Tsunetsugu-Yokota, and Manabu Ato for technical support; and Ryoko Itami for secretarial assistance.

Conflicts of interest statement

The authors declared no conflicts of interest.

References

1 Li, Q., Guan, X., Wu, P., *et al.* 2020. Early Transmission Dynamics in Wuhan, China, of Novel Coronavirus-Infected Pneumonia. *N. Engl. J. Med.* 382:1199.

2 Zhu, N., Zhang, D., Wang, W., *et al.* 2020. A Novel Coronavirus from Patients with Pneumonia in China, 2019. *N. Engl. J. Med.* 382:727.

3 Zhou, P., Yang, X. L., Wang, X. G., *et al.* 2020. A pneumonia outbreak associated with a new coronavirus of probable bat origin. *Nature* 579:270.

4 Wu, F., Zhao, S., Yu, B., *et al.* 2020. A new coronavirus associated with human respiratory disease in China. *Nature* 579:265.

5 Coronaviridae Study Group of the International Committee on Taxonomy of, V. 2020. The species Severe acute respiratory syndrome-related coronavirus: classifying 2019-nCoV and naming it SARS-CoV-2. *Nat. Microbiol.* 5:536.

6 Wu, Z. and McGoogan, J. M. 2020. Characteristics of and Important Lessons From the Coronavirus Disease 2019 (COVID-19) Outbreak in China: Summary of a Report of 72314 Cases From the Chinese Center for Disease Control and Prevention. *JAMA* 323:1239.

7 Guan, W. J., Ni, Z. Y., Hu, Y., *et al.* 2020. Clinical Characteristics of Coronavirus Disease 2019 in China. *N. Engl. J. Med.* 382:1708.

8 Idogawa, M., Tange, S., Nakase, H., and Tokino, T. 2020. Interactive Web-based Graphs of Coronavirus Disease 2019 Cases and Deaths per Population by Country. *Clin. Infect. Dis.* 71:902.

9 Veglia, F., Perego, M., and Gabrilovich, D. 2018. Myeloid-derived suppressor cells coming of age. *Nat. Immunol.* 19:108.

10 Goh, C., Narayanan, S., and Hahn, Y. S. 2013. Myeloid-derived suppressor cells: the dark knight or the joker in viral infections? *Immunol. Rev.* 255:210.

11 Bueno, V., Sant'Anna, O. A., and Lord, J. M. 2014. Ageing and myeloid-derived suppressor cells: possible involvement in immunosenescence and age-related disease. *Age (Dordr)* 36:9729.

12 Garg, A. and Spector, S. A. 2014. HIV type 1 gp120-induced expansion of myeloid derived suppressor cells is dependent on interleukin 6 and suppresses immunity. *J. Infect. Dis.* 209:441.

13 Fang, Z., Li, J., Yu, X., *et al.* 2015. Polarization of Monocytic Myeloid-Derived Suppressor Cells by Hepatitis B Surface Antigen Is Mediated via ERK/IL-6/STAT3 Signaling Feedback and Restrains the Activation of T Cells in Chronic Hepatitis B Virus Infection. *J. Immunol.* 195:4873.

14 Dominguez, C., McCampbell, K. K., David, J. M., and Palena, C. 2017. Neutralization of IL-8 decreases tumor PMN-MDSCs and reduces mesenchymalization of claudin-low triple-negative breast cancer. *JCI Insight* 2:e94296.

15 Zhang, X., Tan, Y., Ling, Y., *et al.* 2020. Viral and host factors related to the clinical outcome of COVID-19. *Nature* 583:437.

16 Li, S., Jiang, L., Li, X., *et al.* 2020. Clinical and pathological investigation of patients with severe COVID-19. *JCI Insight* 5:e138070.

17 Bordoni, V., Sacchi, A., Cimini, E., *et al.* 2020. An inflammatory profile correlates with decreased frequency of cytotoxic cells in COVID-19. *Clin. Infect. Dis.*:ciaa577.

18 Agrati, C., Sacchi, A., Bordoni, V., *et al.* 2020. Expansion of myeloid-derived suppressor cells in patients with severe coronavirus disease (COVID-19). *Cell Death Differ.* 27:3196.

19 Schulte-Schrepping, J., Reusch, N., Paclik, D., *et al.* 2020. Severe COVID-19 Is Marked by a Dysregulated Myeloid Cell Compartment. *Cell* 182:1419.

20 Silvin, A., Chapuis, N., Dunsmore, G., *et al.* 2020. Elevated Calprotectin and Abnormal Myeloid Cell Subsets Discriminate Severe from Mild COVID-19. *Cell* 182:1401.

21 Sacchi, A., Grassi, G., Bordoni, V., *et al.* 2020. Early expansion of myeloid-derived suppressor cells inhibits SARS-CoV-2 specific T-cell response and may predict fatal COVID-19 outcome. *Cell Death Dis.* 11:921.

22 Ministry of Health, Labour and Welfare, Japan. 2020. COVID-19 medical guideline. Available at: https://www.mhlw.go.jp/content/000668291.pdf.

23 Bronte, V., Brandau, S., Chen, S. H., *et al.* 2016. Recommendations for myeloid-derived suppressor cell nomenclature and characterization standards. *Nat. Commun.* 7:12150.

24 Takahashi, T., Ellingson, M. K., Wong, P., *et al.* 2020. Sex differences in immune responses that underlie COVID-19 disease outcomes. *Nature* 588:315.

25 Ellinghaus, D., Degenhardt, F., Bujanda, L., *et al.* 2020. Genomewide Association Study of Severe Covid-19 with Respiratory Failure. *N. Engl. J. Med.* 383:1522.

26 Fidel, P. L., Jr. and Noverr, M. C. 2020. Could an Unrelated Live Attenuated Vaccine Serve as a Preventive Measure To Dampen Septic Inflammation Associated with COVID-19 Infection? *mBio* 11:e00907.

27 Ioannou, M., Alissafi, T., Lazaridis, I., *et al.* 2012. Crucial role of granulocytic myeloid-derived suppressor cells in the regulation of central nervous system autoimmune disease. *J. Immunol.* 188:1136.

28 Dilek, N., Vuillefroy de Silly, R., Blancho, G., and Vanhove, B. 2012. Myeloid-derived suppressor cells: mechanisms of action and recent advances in their role in transplant tolerance. *Front. Immunol.* 3:208.

29 Esher, S. K., Fidel, P. L., Jr., and Noverr, M. C. 2019. Candida/Staphylococcal

Polymicrobial Intra-Abdominal Infection: Pathogenesis and Perspectives for a Novel Form of Trained Innate Immunity. *J. Fungi (Basel)* 5:37.

30 Horby, P., Lim, W. S., Emberson, J. R.*, et al.* 2020. Dexamethasone in Hospitalized Patients with Covid-19 - Preliminary Report. *N. Engl. J. Med.*:NEJMoa2021436.

31 Biran, N., Ip, A., Ahn, J.*, et al.* 2020. Tocilizumab among patients with COVID-19 in the intensive care unit: a multicentre observational study. *Lancet Rheumatol.* 2:e603.

32 Guaraldi, G., Meschiari, M., Cozzi-Lepri, A.*, et al.* 2020. Tocilizumab in patients with severe COVID-19: a retrospective cohort study. *Lancet Rheumatol.* 2:e474.

33 Xu, X., Han, M., Li, T.*, et al.* 2020. Effective treatment of severe COVID-19 patients with tocilizumab. *Proc. Natl. Acad. Sci. U S A* 117:10970.

Figure Legends

Fig. 1: Identification of myeloid-derived suppressor cells (MDSCs) in COVID-19 patients.

(A) Gating strategy used to identify each MDSC subset are shown. After selection of singlet cells and gating of whole white blood cells, lineage marker (CD3, CD19, CD56) negative and HLA-DR$^{-/lo}$CD11b^{+}CD33^{+} cells were identified as MDSCs among live 7-AAD^{-} cells. CD14^{-} CD15^{-}, CD14^{+}CD15^{-}, and CD14^{-}CD15^{+} MDSCs were defined as e-MDSCs, M-MDSCs, and PMN-MDSCs, respectively. (B) Representative plots of MDSC subsets in healthy donors and COVID-19 patients with different severity of symptoms (mild case, M-006 day 20; moderate I case, MI-001 day 18; moderate II case, MII-007 day 17; severe surviving case, S-001 day 20; severe fatal case, F-005 day 16) are shown. (C) The frequencies of PMN-MDSCs relative to live PBMCs (7-AAD^{-} whole PBMCs) at different time points were analyzed. Each symbol indicates individual patients described at the right side of the plot.

Fig. 2: Analysis of the frequencies of MDSC subsets in COVID-19 patients.

The frequencies of each MDSC subset relative to live PBMCs (7-AAD^{-} whole PBMCs) were analyzed for the first 3 weeks (day 0–21 after symptom onset). Data are represented as points indicating the data of independent samples and the mean (bar) ± SD of independent samples. Healthy donors, n = 7, n’ = 7. COVID-19 mild cases, n = 21, n’ = 12; moderate I cases, n = 19, n’ = 7; moderate II cases, n = 21, n’ = 8; severe surviving cases, n = 12, n’ = 7; severe fatal cases, n = 7, n’ = 5 (n, samples; n’, individuals). Two-way ANOVA and Tukey’s post-hoc test were performed for statistical analysis (***$p < 0.001$, ****$p < 0.0001$).

Fig. 3: Analysis of plasma cytokines/chemokines in COVID-19 patients.

Concentrations of plasma cytokines/chemokines were analyzed for the first 3 weeks (day 0–21 after symptom onset). Data are shown as points indicating the data of independent samples and the mean (bar) ± SD of independent samples. Healthy donors, n = 7, n' = 7. COVID-19 mild cases, n = 21, n' = 12; moderate I cases, n = 19, n' = 7; moderate II cases, n = 21, n' = 8; severe surviving cases, n = 12, n' = 7; severe fatal cases, n = 7, n' = 5 (n, samples; n', individuals). One-way ANOVA and Tukey's post-hoc test were performed for statistical analysis (**$p < 0.01$, ***$p < 0.001$, ****$p < 0.0001$).

Fig. 4: Associations between MDSC subsets and plasma IL-8 levels.

Correlations between plasma IL-8 concentrations and frequencies of e-MDSCs, M-MDSCs, or PMN-MDSCs relative to live PBMCs were analyzed. Healthy donors, n = 7, n' = 7; COVID-19 mild cases, n = 27, n' = 12; moderate I cases, n = 24, n' = 7; moderate II cases, n = 29, n' = 8; severe surviving cases, n = 20, n' = 8; severe fatal cases, n = 7, n' = 5 (n, samples; n', individuals). Spearman's rank correlation coefficients, *p* values, and linear regression lines are indicated in plots. Correlations with $|r| > 0.4$ and $p < 0.01$ were considered significant.

Fig. 1

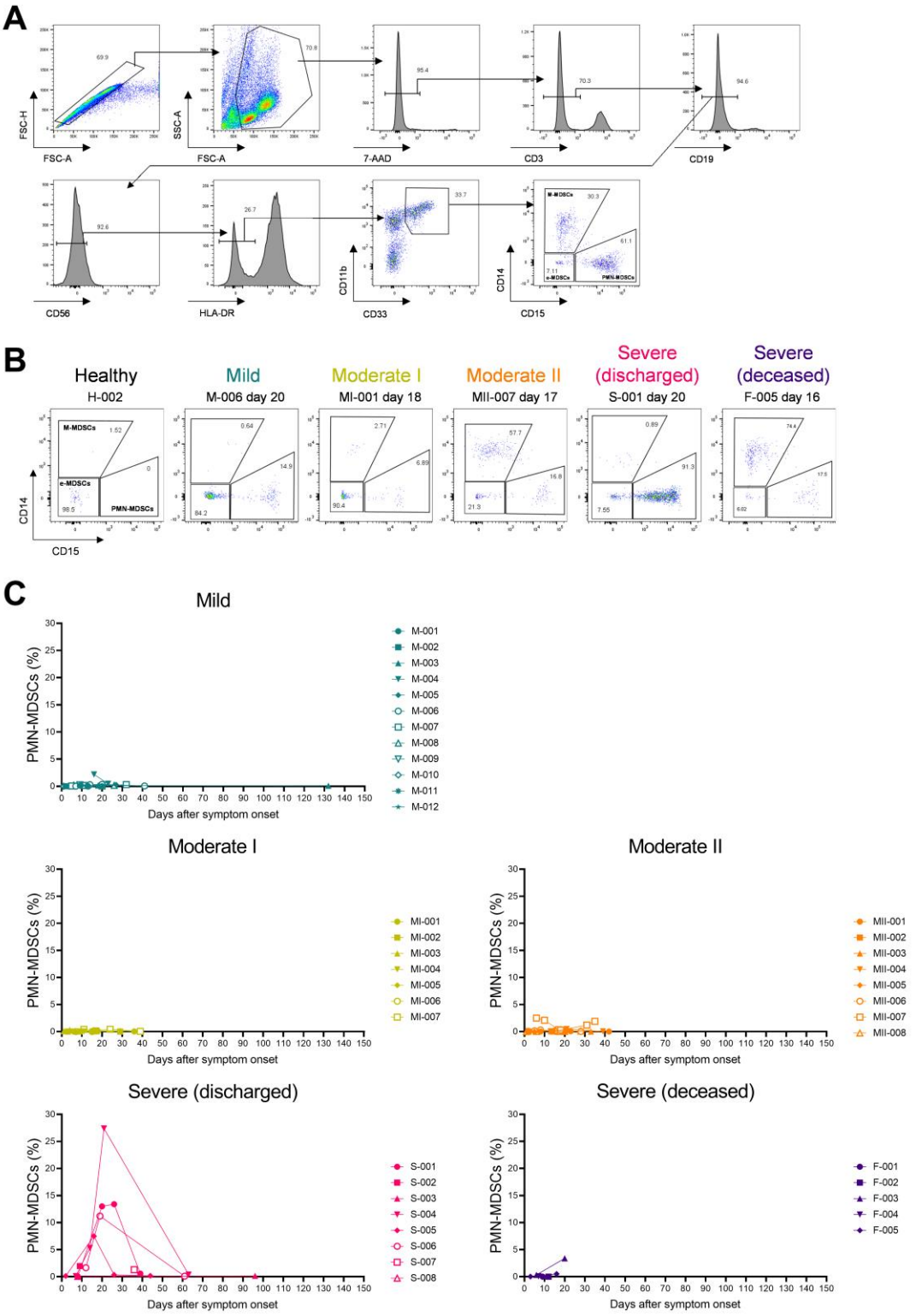
A
FSC-H
FSC-A
SSC-A
FSC-A
7-AAD
CD3
CD19
CD56
HLA-DR
CD11b
CD33
CD14
CD15
B
Healthy
H-002
Mild
M-006 day 20
Moderate I
MI-001 day 18
Moderate II
MII-007 day 17
Severe (discharged)
S-001 day 20
Severe (deceased)
F-005 day 16
M-MDSCs
e-MDSCs
PMN-MDSCs
CD14
CD15
C
Mild
Moderate I
Moderate II
Severe (discharged)
Severe (deceased)
PMN-MDSCs (%)
Days after symptom onset
M-001
M-002
M-003
M-004
M-005
M-006
M-007
M-008
M-009
M-010
M-011
M-012
MI-001
MI-002
MI-003
MI-004
MI-005
MI-006
MI-007
MII-001
MII-002
MII-003
MII-004
MII-005
MII-006
MII-007
MII-008
S-001
S-002
S-003
S-004
S-005
S-006
S-007
S-008
F-001
F-002
F-003
F-004
F-005

Fig. 2

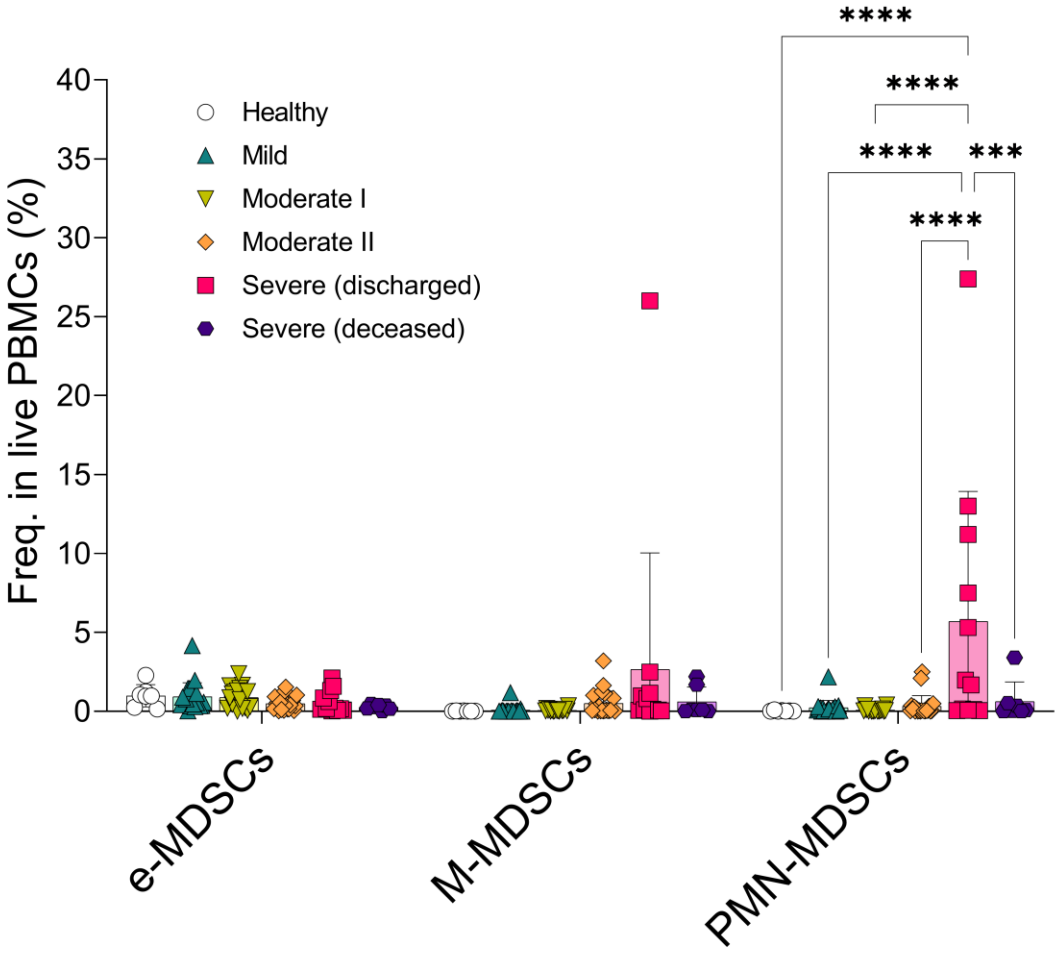
****
****
****
***
****
Healthy
Mild
Moderate I
Moderate II
Severe (discharged)
Severe (deceased)
Freq. in live PBMCs (%)
40
35
30
25
20
15
10
5
0
e-MDSCs
M-MDSCs
PMN-MDSCs

Fig. 3

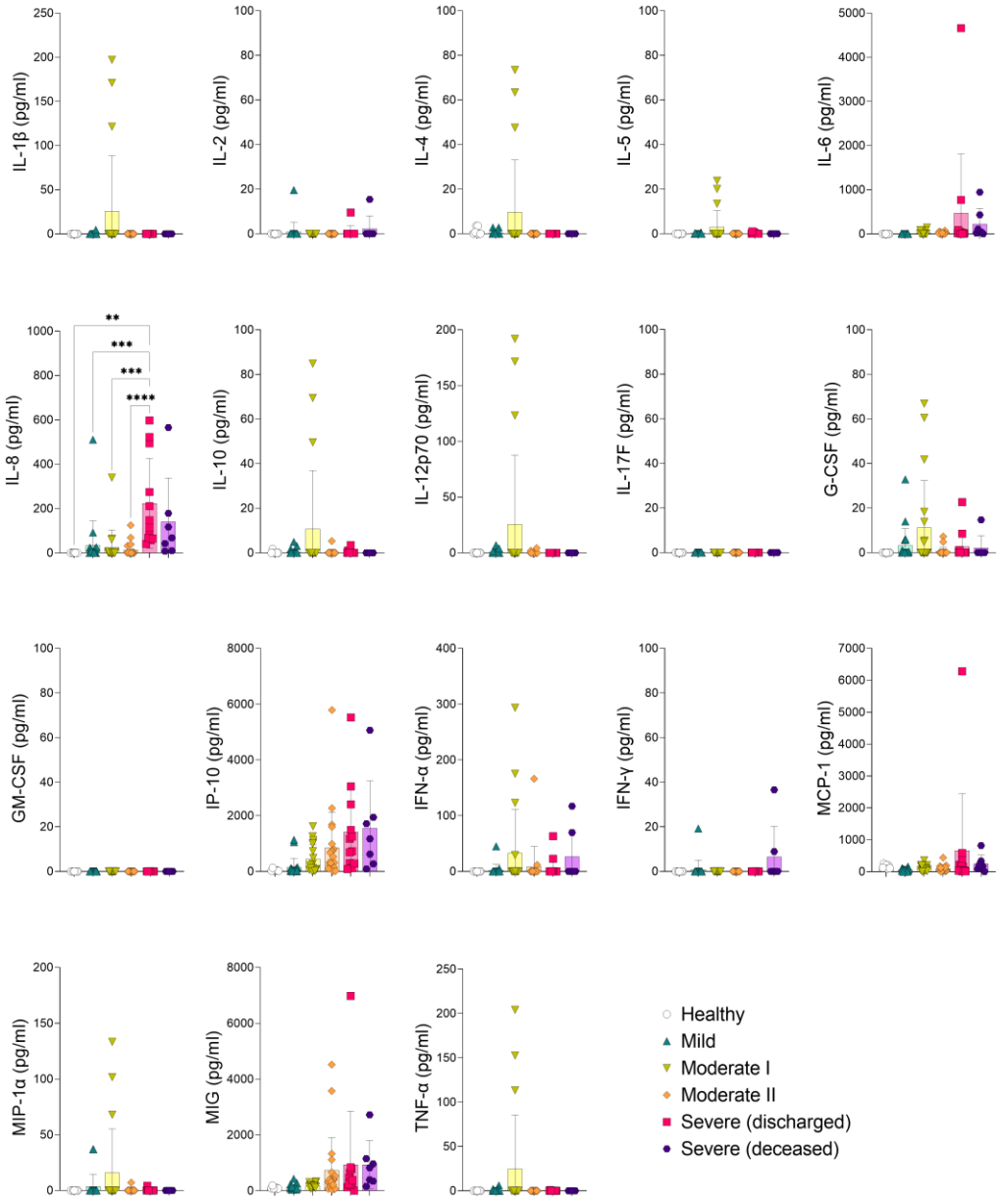
IL-1β (pg/ml)
IL-2 (pg/ml)
IL-4 (pg/ml)
IL-5 (pg/ml)
IL-6 (pg/ml)
IL-8 (pg/ml)
**
***
***
****
IL-10 (pg/ml)
IL-12p70 (pg/ml)
IL-17F (pg/ml)
G-CSF (pg/ml)
GM-CSF (pg/ml)
IP-10 (pg/ml)
IFN-α (pg/ml)
IFN-γ (pg/ml)
MCP-1 (pg/ml)
MIP-1α (pg/ml)
MIG (pg/ml)
TNF-α (pg/ml)
Healthy
Mild
Moderate I
Moderate II
Severe (discharged)
Severe (deceased)

Fig. 4

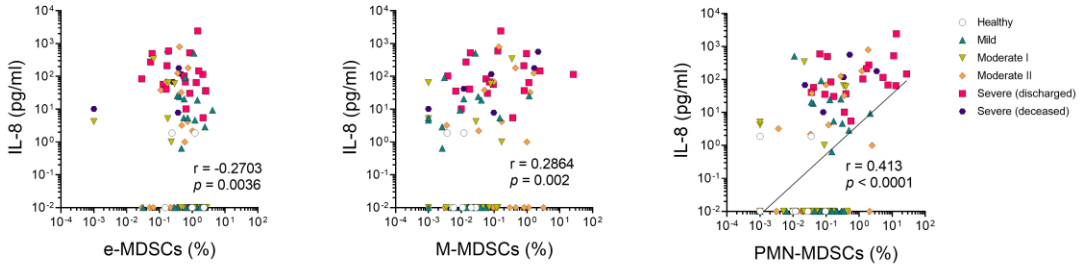
IL-8 (pg/ml)
e-MDSCs (%)
r = -0.2703
p = 0.0036
M-MDSCs (%)
r = 0.2864
p = 0.002
PMN-MDSCs (%)
r = 0.413
p < 0.0001
Healthy
Mild
Moderate I
Moderate II
Severe (discharged)
Severe (deceased)